# APPLICATION OF SCALE RESOLUTION MODELS FOR IRIS PATTERN SEGMENTATIONS BASED ON EDGE DETECTIONS

**by**

**D. I. Lanlege & Imoni. S. O,**

*Department of Mathematical Sciences, Federal University Lokoja Kogi State, Nigeria.*

*Email: loislanlege@yahoo.com david.lanlege@fulokoja.edu.ng, Sunday.imoni@fulokoja.edu.ng*

## Abstract

*This paper considers scale resolution models for iris pattern segmentations based on edge detections. Edges in images can be mathematically defined as local singularities. Until recently, the Fourier transform was the main mathematical tool for analysing singularities. However, the Fourier transform is global and as such not well adapted to local singularities and it is hard to find the location and spatial distribution of singularities with Fourier transforms. It shows how vibration could be further minimized in the improved Mixed Radix Algorithm, by deriving a numerical algorithm for noise minimization in signal processing systems for faster pattern recognition. It is also proved analytically that this derived algorithm for noise minimization converges.*

**Keywords***: Scale Resolution Model, Pattern Segmentation, Edge Detection, Singularities and Fourier Transform*.

## 1.0 Introduction

A very common source of degradation in a digital image is noise contamination. Noise may be present in an image due to different reasons and its effect in degrading the image is different for different kinds of noise. The image corrupted with noise generally suffer from having low signal-to-noise ratio and may not be suitable for further processing without removing or reducing the effect of noise in it. For example, a biomedical image corrupted with noise cannot be used reliably for clinical diagnosis of disease. A satellite image corrupted with speckle noise fails to represent the remote-sensed data of, say, a geographical terrain. Hence removal of noise from the image is of utmost importance in image processing and analysis.

However, removal of noise like every known noise cleaning algorithm is associated with partial removal of the desired signal component. For example, mean filters generally blur the edges and the comer points present in the image [1].

Signature recognition is defined as the process of verifying the writer's identity by checking his/her signature against samples kept in a database. The result of this process is usually a number between 0 and 1 which represents a fit ratio (1 for match and 0 for mismatch) [2]. The threshold used for the confirmation/rejection decision depends on the nature of the application. The distinctive biometric patterns of this modality are the personal rhythm, acceleration and pressure flow when a person types a specific word or group of words (usually the hand signature of the individual).

This paper is aimed applying scale resolution models that will enable us carry out Iris Pattern Segmentations based on edge detections. The general mathematical construct is:

$$\frac{1}{\pi\left(r_i^2 - r_p^2\right)}\int_0^{\pi/2}\int_{r_p}^{r_i}\left(\frac{\delta}{r}\right)sin(\theta)rdrd\theta = \frac{4}{\pi}\frac{\delta}{r_i + r_p} \qquad (1)$$

Some of the methods and the results in edge detection are:

## 2.0 Edge Detector Using Wavelets

Wavelet transforms provide a local analysis; they are especially suitable for time-frequency analysis [7] such as for singularity detection problems. With the growth of wavelet theory, the wavelet transforms have been found to be remarkable mathematical tools to analyse the singularities including the edges, and further, to detect them effectively. Mallat and Zhong [8] proved that the maxima of the wavelet transform modulus can detect the location of the irregular structures. The wavelet transform characterizes the local regularity of signals by decomposing them into elementary building blocks that are well localised both in space and frequency. This not only explains the underlying mechanism of classical edge detectors, but also indicates a way of constructing optimal edge detectors under specific working conditions.

A remarkable property of the wavelet transform is its ability to characterize the local regularity of functions. For an image $f(x, y)$, its edges correspond to singularities of $f(x, y)$, and thus are related to the local maxima of the wavelet transform modulus. Therefore, the wavelet transform can be used as an effective method for edge detection.
Assume $f(x, y)$ is a given image of size $M \times N$.At each scale $j$ with $j > 0$ and$S_0 f = f(x, y)$ the wavelet transform decomposes $S_{j-1}f$ into three wavelet bands: a low-pass band $S_j f$, a horizontal high-pass band $W_j^H f$ and a vertical high-pass band.
$W_j^V f$ The three wavelet bands ($S_j f$ $W_j^V f$ $W_j^H f$ ) at scale j are of size $M \times N$, which is the same as the original image, and all filters used at scale $j$ ($j > 0$) are up sampled by a factor of $2^j$compared with those at scale zero. In addition, the smoothing function used in the construction of a wavelet reduces the effect of noise. Thus, the smoothing step and edge detection step are combined together to achieve the optimal result. The short coming of this method is that the smoothing wavelet to reduce Noise cannot effectively remove the noise and Occlusion of the eye and this makes it difficult to segment Iris.

## 3.0 Filter Bank Gabor

The processing of facial images by a Gabor filter has been widely used for its biological relevance and technical properties. The Gabor filter kernels have similar shapes as the receptive fields of simple cells in the primary visual cortex. They are Multiscale and multi-orientation kernels. The Gabor transformed face images yield features that display scale, locality and differentiation properties. These properties are quite robust to variability of face image formation, such as the variations of illumination, head rotation and facial expressions.

## 4.0 Gabor Functions and Wavelets

The two-di1mensional Gabor Wavelets function $g(x, y)$and its Fourier transform $G(u, v)$ can be defined as follows:

$$G(x, y) \frac{1}{2\pi\sigma_x\sigma_y} \ell XP\left[-\frac{1}{2}\left(\frac{X^2}{\sigma_X^2} + \frac{Y^2}{\sigma_Y^2}\right) + 2\pi lwx\right] \quad (2)$$

$$G(\mu, v) = \ell XP\left[-\frac{1}{2}\left(\frac{(\mu - w)^2}{\sigma_\mu^2} + \frac{v^2}{\sigma_v^2}\right)\right] \quad (3)$$

Where $\sigma\mu = \frac{1}{2}\pi\sigma_x$ and $\sigma_v = \frac{1}{2}\pi\sigma y$ . Gabor functions can form a complete but non-orthogonal basis set. Expanding a signal using this basis provides localised frequency description. A class of self-similar functions, referred to as Gabor wavelets in the following discussion, is now considered. Let $g(x, y)$ be the mother Gabor wavelet, then this self-similar filter dictionary can be obtained by appropriate dilations and rotations of $g(x,y)$ through the generating function:

$$g_{mn}(x,y) = a^{-m}G(x,y) \tag{4}$$

$$x = a^{-m}(x\,cos\theta + y sin\theta) \tag{5}$$

$$y = a^{-m}(-x\,sin\theta + y cos\theta) \tag{6}$$

Where $a > 1$, $m, n$ = integer and $\theta = n\pi/k$ is the orientation ($k$ is the number of orientations) and $a^{-m}$ is the scale factor.

## 5.0 Gabor Filter Dictionary Design

The non-orthogonality of the Gabor wavelets implies that there is redundant information in the filtered images, and the following strategy is used to reduce this redundancy.

Let $U_i$ and $U_h$denote the lower and upper centre frequencies of interest.

Let K be the number of orientations and S be the number of scales in the Multiresolution decomposition. As proposed by [3] the design strategy is to ensure that the half-peak magnitude support of the filter responses in the frequency spectrum touch each other. This result in the following formulas for computing the filter parameters $\sigma\mu$and $\sigma v$(and thus $\sigma x$and $\sigma y$:

$$a = \left(\frac{U_h}{U_t}\right)^{-\frac{1}{s-1}} \tag{7}$$

$$\sigma_{mu} = \frac{(a-1)U_h}{(a+1)\sqrt{2In(2)}} \tag{8}$$

$$\sigma_v = tan\left(\frac{\pi}{2k}\right)\left[U_h - 2In\left(\frac{2\sigma_\mu^2}{U_h}\right)\right]\left[2In(2) - \frac{[2In(2)]^2\sigma^2\mu}{U_h^2}\right] \tag{9}$$

where $W = U_h\ and\ m = 0,1, \dots S-1$.To eliminate the sensitivity of the filter response to absolute intensity values, the real (even) components of the $2D$Gabor filters are biased by adding a constant to make them zero mean.

## 6.0 Augmented Gabor-Face Vector

Given any image $I(x,y)$,its Gabor wavelet transformation is

$$W_{mn} = \int 1(x_1, y_1)\, g_{mn}^*(x - x_1, y - y_1)dx_1dy_1 \tag{10}$$

Where $g_{mn}$indicates the complex conjugate of $g_{mn}$. The Gabor wavelet transformation of the facial image is calculated at S scales $m\epsilon\{0,1,2, \dots S\}$and K different orientations, $n\epsilon\{0,1,2, \dots K\}$and let us set$U_1 = 0.05$ and $U_h = 0.4$.

$W_{mn}$denotes a Gabor wavelet transformation of a face image at the scale m and orientation *n*. shows a sample face image from the database and its forty filtered images (five scales: $S = 5$ and eight orientations: $K = 8$have been taken).The augmented Gabor-face vector can then be defined as follows:

$$x = \left(W_{0,0\dots}^t W^t S_{,k}\right)^t \tag{11}$$

Where *t*, is the transpose operator. The augmented Gabor-face vector can encompass all facial Gabor wavelet transformations, and has important discriminatory information that can be used in the classification step

## 7.0 The Conjugate Gradient Algorithm

The back propagation algorithm was the first and until recently the only algorithm to train feed forward multiplayer perceptrons. We here present the CGM variant.

Until recently, when the extended conjugate gradient method (ECGM) was formulated, the conjugate gradient method (CGM) has been one of the most effective method among the iterative methods for solving linear system of equations (of the form in equation(11) as a minimization method. The CGM provides faster convergence for quadratic functional than gradient descent methods while avoiding computation of the inverse of the Hessain matrix.

**Materials and Methods**

Since R is a positive definite, real symmetric n x n matrix, then the quadratic functional

$$F(W) = \frac{1}{2} w^T R w - w^T P + C \tag{12}$$

Has a unique minimum point w* which is a solution of the system of equations Qx = b.

Since $\nabla f(X) = \mathrm{Q_X} - \mathrm{b}$

Then we can write

$$\mathrm{Qx} * = \mathrm{b} \tag{13}$$

The minimization iteration updating method for (12) is given as

$$\mathrm{W_{k+1}} = \mathrm{W_k} + \alpha_\mathrm{k}(\mathrm{Rw_k} - \mathrm{P}) \tag{14}$$

Where

$$\alpha_\mathrm{k} = \frac{(\nabla \mathrm{f}(\mathrm{x_k}))^\mathrm{T} \mathrm{d_k}}{\mathrm{d_k^T Q d_k}} \tag{15}$$

The value of the step size $\alpha_\mathrm{k}$that minimizes $f(X_{k+1})$ can be found by setting

$$\frac{df(x_k - \alpha_k(Qk_x - b))}{d\alpha_k} = O, \tag{16}$$

yielding

$$\alpha_\mathrm{k} = \frac{(Qk_x - b)^T (Qk_x - L)}{(Qk_x - b)^T (Qk_x - b)} \tag{17}$$

With the step size $\alpha_\mathrm{k}$ chosen as in equation (17), we have the following important result on the convergence rate of the gradient descent method.

**8.0 The Active Contour Model**

In active contour model, we use the technique of matching a deformable model to an image by means of energy minimization. An active contour model inhalized near the target refined iteratively and is attracted towards the salient contour. A snake in the image can be represented as a set of n points.

$$V_i = h(x_i, y_i) \tag{18}$$

Where $i = 0, \dots, n-1$

We can write the energy function as:

$$\begin{aligned} \mathrm{E^*_{snake}} &= \int_0^1 \mathrm{E_{in} V(S) ds} \\ &\quad + \int_0^1 \mathrm{E_{image} V(S) ds} + \int_0^1 \mathrm{E_{con}\, V(S) ds} \end{aligned} \tag{19}$$

$$\begin{aligned} \mathrm{E^*_{snake}} &= \int_0^1 (\mathrm{E_{in}} + \mathrm{E_{image}} \\ &\quad + \mathrm{E_{con}}) \mathrm{V(S) ds} \end{aligned} \tag{20}$$

$$\mathrm{E_{ex}} = \mathrm{E_{Image}} + \mathrm{E_{con}}$$

(21)

Where, $E_{in}$ denote internal energy of the Spline (snakes) due to bending.
$E_{image}$ denotes the image forces acting on Spline
$E_{con}$ denote external constraint force introduced by user
The combination of $E_{image}$ and $E_{con}$ can be represented as $E_{ex}$ that denotes the external energy acting on the Spline.
V(s) vector representing the Spline
Internal energy of the snake as given by [4] is

$$E_{in} = E_{cont} + E_{cur}$$

Where $E_{cont}$ denotes the energy of the snake contour.
$E_{cur}$ denotes the energy of the Spline curvature.
By finite difference notation:

$$\frac{dV}{ds} \approx V_{i+1} - V_i \tag{22}$$

$$\frac{d^2V}{ds^2} \approx (V_{i+1} - V_i) - (V_i - V_{i-1}) \tag{23}$$

$$= V_{i+1} - 2V_i + V_{i-1} \tag{24}$$

$$E_{in} = (\alpha(s)|V_S(s)|^2 + \beta(s)|V_{ss}(s)|^2) = \frac{\left(\alpha(s)\left\|\frac{d\bar{v}}{ds}(s)\right\|^2 + \beta(s)\left\|\frac{d^2\bar{v}}{ds^2}(s)\right\|^2\right)}{2}$$

$$E_{in} = \sum_{i=0}^{n-1} \underbrace{\alpha(s)|V_{i+1} - V_i|^2}_{\text{Elasticity}} + \underbrace{\beta(s)|V_{i+1} - 2V_i + V_{i-1}|^2}_{\text{stiffness}}$$

Where α(s) regulates internal energy of the Spline
β (s) regulates and develops the move curves of the Spline
The first-order term makes the snake act like a membrane and second-order term makes it act like a thin plate. Large values of α (s) will increase the internal energy of the snake as it stretches more and more, whereas small value of α (s) will make the energy function insensitive to the amount of stretch. Similarly, large values of $\beta$(s) will increase the internal energy of the snake as it develops more curves, whereas small values of $\beta$ (s) will make the energy function insensitive to curves in the snake. Smaller values of both α (s) and $\beta$ (s) will place fewer constraints on the size and shape of the snake.
According to Goswami [5], we introduce$(G_{x,y})$ as the gradient of the image and we have

$$E_{ex} = -\sum_i |G_x((x_i, y_i)|^2 + \left|G_y(x_i, y_i)\right|^2) \tag{26}$$

$$G_x = \frac{\partial}{\partial} G_\delta \otimes I \tag{27}$$

$$G_y = \frac{\partial}{\partial} G_\delta \otimes I \tag{28}$$

Where $G(x, y)$is the gradient image of the Spline
We introduce the forward difference operator in order to move the gradient line to the region of interest.

$$E_{edge} = \left|\nabla\left(G(x, y) * I(x, y)\ \right)\right|^2 \tag{29}$$

Where

$$\nabla \equiv \left(\frac{\partial}{\partial x}, \frac{\partial}{\partial y}\right) \tag{30}$$

and

$$G(x,y)=\frac{1}{\sqrt{2\pi\sigma^2}}e^{-\frac{(x-x_c)^2+(y-y_c)^2}{2\sigma^2}} \qquad (31)$$

$G(x,y)$ is a Gaussian smoothing function with scaling parameter $\sigma$ to select the proper scale of edge analysis. The edge map is then used in a voting process to maximize the defined Hough transform.

$$\mathrm{H}(\mathrm{x_c},\mathrm{y_c},\mathrm{r})=\sum_{\mathrm{i}=1}^{\mathrm{n}}\mathrm{h}(\mathrm{x_i},\mathrm{y_{i,}}\mathrm{x_c},\mathrm{y_c},\mathrm{r}) \qquad (32)$$

As a standard image analysis tool used for finding curves that can be defined in a parametrical form such as lines and circles.[5] Maximum point in the Hough space corresponds to the radius r and centre coordinate $x_c$ and $y_c$ of the circle best defined by the edge points

$$(x_i,y_i)\ \forall\ i=1,\dots,n \qquad (33)$$

$$\mathrm{H}(\mathrm{x_c},\mathrm{y_c},\mathrm{r})=\sum_{\mathrm{i}=1}^{\mathrm{n}}\mathrm{h}(\mathrm{x_i},\mathrm{y_{i,}}\mathrm{x_c},\mathrm{y_c},\mathrm{r}) \qquad (34)$$

Where $H(x_c,y_c,\ r)$ shows a circle through a point, the coordinates of $x\ _c,y_c,\ r$ define a circle

$$x_c^2+y_c^2+r^2=0 \qquad (35)$$

For edge detection for iris boundaries the above equation becomes

$$(x_i-x_c)^2+(y_i-y_c)^2-r^2=0 \qquad (36)$$

**Simple Elastic Curve**

For a curve represented as a set of points a simple elastic energy term is

$$E_{in}=\alpha(s)\sum_{i=0}^{n-1}L_i^2 \qquad (37)$$

$$Ein=\ \alpha(s)\sum_{i=0}^{n-1}(x_{i+1}-x_i)^2+(y_{i+1}-y_i)^2 \qquad (38)$$

Where $L_i^2$ is the internal elastic component and α(s) control the internal elasticity of the curves

This makes the curve to shrink to a point (like a very small elastic band).

$$E_{total}(v_0,\cdots,v_{n-1})=-\sum_{i=0}^{n-1}\|G(v_i)\|^2+\alpha(s)\sum_{i=0}^{n-1}\|v_{i+1}-v_i\|^2 \qquad (39)$$

$$E_{total}(v_0,\cdots,v_{n-1})=\sum_{i=0}^{n-1}E_i(v_i,v_{i+1}) \qquad (40)$$

Where $\mathrm{E}_i(V_i,V_{i+1})=-\|G(v_i)\|^2\ +\alpha(s)\|v_{i+1}-v_i\|^2$

$E_{total}$ can also be represented based on the concept of the expression derived by [6]

$$E_{total}\ =E_{in}+E_{ex} \qquad (41)$$

Next, our work introduces$\alpha(s)$ as the strength of the internal elastic component which can be controlled, i.e

$$E_{in}=\ \alpha(s)\sum_{i=0}^{n-1}(L_i)^2 \qquad (42)$$

or

$$E_{in} = \alpha(s)\sum_{i=0}^{n-1} L_i^2 \quad (43)$$

By dynamic programming, energy is minimized, that is (43) is iterated until optimal position for each point in the centre of the iris i.e. the snake is optimal in the local search space constrained

$$E(V_1, V_2, \dots, V_n,), = E_1(V_1, V_2) + E_2(V_2, V_3) + \ \dots + \ E_{n-1}(V_{n-1}, V_n) \quad (44)$$

Curvature of level lies in a slightly smoothed image is used to detect corners and terminations in an image. Now,

Let C $(x, y)$ = G$\sigma *$ $I(x, y)$ (45)

be a slightly smoothened version of the image.

C = curvature of the image

$Let\ \theta = tan^{-1}\left(\frac{C_y}{C_x}\right)$ be the gradient of the image, where $C_x$ and $C_y$ are the coordinates of the pupil.

$\theta$ = Angle between the images of the curvatures

And let n = (cos$\theta$, sin$\theta$) be unit vector along the gradient direction

$\frac{dn}{d\theta}$= (- sin$\theta$, cos$\theta$) be unit vector along the perpendicular to the gradient direction.

The termination function energy $E_{term}$ is represented by

$$E_{term}=\frac{d\theta}{dn} \quad (46)$$

$$E_{term} = \frac{d\theta}{dn} = \frac{d^2C/d^2n}{dC/dn} = \frac{C_{yy}C_x^2 - 2C_{xy}C_xC_y + C_{xx}C_y^2}{\left(C_x^2 + C_y^2\right)^{3/2}} \quad (47)$$

Constraint energy of some system, including the original snakes' implementation, allowed for user interaction to guide the snakes, not only in initial placement but also in their energy terms. Such constraint energy $E_{con}$ can be used to interactively guide the snakes towards or away from particular features

**Illustration**

Find the area enclosed by the curve $r = 1 + cos\theta$ and the radius vectors at $\theta = 0\ and\ \theta = \pi/2$

$$A = \frac{1}{2}\int_0^{\pi/2} r^2\, d\theta = \frac{1}{2}\int_0^{\pi/2} (1 + 2cos\theta\ + cos^2\theta)d\theta \quad (48)$$

$$= \frac{1}{2}\left[\theta + 2sin\theta + \frac{\theta}{2} + \frac{sin2\theta}{4}\right]_0^{\pi/2} \quad (49)$$

$$= \frac{1}{2}\left\{\left(\frac{3\pi}{4} + 2 + 0\right) - (0)\right\} \quad (50)$$

$$\therefore = \frac{3\pi}{8} + 1 = 2.178 \quad (51)$$

So the area of a polar sector is easy enough to obtain. It is simply

$$A = \int_{\theta_1}^{\theta_2} \frac{1}{2} r^2 d\theta \quad (52)$$

To find the volume generated when the plane figure bound by $r = f(\theta)$ and the radius vectors at $\theta = \theta_1$ and $\theta = \theta_2$, rotates about the initial line.

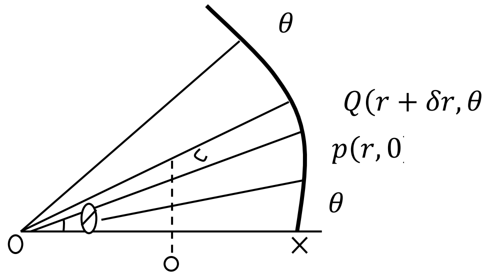


**Figure 1**The volume of plane figure bounded by the polar curve

If we regard the elementary sector OPQ as approximately equal to the $\nabla OPQ$ the centroid C is distance 2r/3 from O.

We have: Area $OPQ \approx \frac{1}{2}r(r+\delta r)sin\delta\theta$

Volume generated when OPQ rotates about $OX = \delta V$

$\therefore$ $\delta V$= area OPQ x distance travelled by its centroid (Pappus)

$= \frac{1}{2}r(r+\delta r)sin\delta\theta.2\pi$.CD (53)

$= \frac{1}{2}r(r+\delta r)sin\delta\theta.2\pi.\frac{2}{3}rsin\theta = \frac{2}{3}\pi r^2(r+\delta r)sin\delta\theta.sin\theta$ (54)

$\therefore \frac{\delta V}{\delta\theta} = \frac{2}{3}\pi r^2(r+\delta r)\frac{sin\delta\theta}{\delta\theta}.sin\theta$ (55)

Then when $\delta\theta \to 0, \frac{dV}{d\theta} =$

(5

$$V = \int_{\theta_1}^{\theta_2} \frac{2\pi r^2}{3} sin\theta d\theta$$

$V = \frac{}{3}\int_{\theta_1} sin\theta d\theta$ (57)

$V = \frac{2\pi r^2}{3}cos\theta \Big|_{\theta_1}^{\theta_2}$ (58)

Correct. This is another standard result.

To find the length of arc of the polar curve r = f($\theta$) between $\theta = \theta_1$and $\theta = \theta_2$

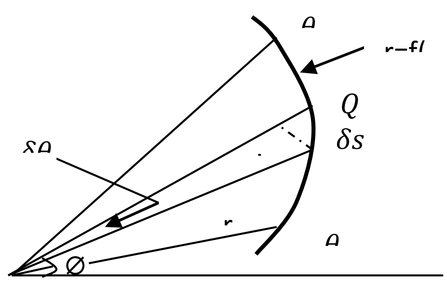


**Figure 2**The length of arc of the polar curve

With the usual figure $\delta s^2 \approx r^2 . \delta\theta^2 + \delta r^2 \therefore \frac{\delta s^2}{\delta\theta^2} \approx r^2 + \frac{\delta s^2}{\delta\theta^2}$ (3) (59)

$$if \delta\theta \to 0, \left(\frac{ds}{d\theta}\right)^2$$

$$= r^2 + \left(\frac{ds}{d\theta}\right)^2 \quad (60)$$

$$\therefore \frac{ds}{d\theta}\sqrt{r^2 + \left(\frac{ds}{d\theta}\right)^2} \quad (61)$$

$$s = \int_{\theta_2}^{\theta_2} \sqrt{r^2} \left(\frac{ds}{d\theta}\right)^2 d\theta \quad (62)$$

In the effort to find a good criterion for characterizing what the "best" function $u$ should be, [6] sort for a criterion to minimize, which corresponds better to the structure of the images. They proposed the consideration of the "Bounded Variation" of the function $u$ as a measure of the optimality of an image. The criterion is approximately the integral $\int_\Omega |\nabla u(x)| dx$ The main advantage is that this integral can be defined for functions that have discontinuities along hyper surfaces (in 2-dimensional images, along 1-dimensional curves), and this is essential to get a correct representation of the edges in images to facilitate pattern recognition The problem to solve is

Minimize $\left\{\int_\Omega |\nabla u(x)| dx\right\}$ (63)

We use the notion of $\mathrm{r} - \mathrm{C}$ onvergence to propose a numerical approach for computing a solution [7] presents the symmetry consideration and by the centering theorem of Fourier transform, we have reinforced the fact that the pixel Number, $N = 2^L$ where $L \in Z^+$, is best in terms of speed, for the FFT and the IFFT operations for image processing for pattern recognition. When $N$ is not a positive integer power of 2, we have modified/ improved the Mixed Radix Algorithm by stretching $N$ to the next integer power of 2, using our established rule for stretching i.e. 0's for even values of $N$ and 1's for odd value of $N$ .when compared with the MATLAB fft ($N$) operator, it clearly shows an improvement in speed, over the Mixed Radix Algorithm.

Refer [7] and [8] $\Gamma -$ convergence is a special notion of convergence that is adapted to variation problems. If one is looking for the minimizes of a function $F(X), x \in X$ (where X is some space) and wants to approximate it with minimizers$(X_n)$ of approximate problem $\min_X \in X, F_n(X)$, One wonders when $(X_n)$ converges to a minimizer of $F$? Considering the classical notion of limits of functions, only the uniform convergence seems suitable to handle this problem. However, this notion of convergence is far too strong for most applications.

**9.0 Conclusion**

In the application of image processing tools, an image is first passed through the PID low pass filter which allows the image intensity to be adjusted by the image intensity adjustment tools. Then, finally sobel edge detector is used to enhance the outline of the image. This order is necessary for the processing because sobel edge detector is very sensitive to noise and needs to be filtered out before the edge detector application. More so, since the gradient of the sobel edge detector is related to the change in intensity at the edge of an object, the image intensity adjustment is used to produce a higher contrast image. As image intensity adjustment can improve the intensity of the image as well as noise within the image, the noise must be filtered out before the intensity adjustment. In [3], Proportional Integral Derivative Controller Filter (PID) is employed to reduce the effect of noise.The new Multiscale Approach method for edge detection was able to detect iris region (pupil, outer boundary circle) using Snake Active Contour and Standard Galerkin Method. This in turn greatly reduces the search for the Hough transform, thereby improving the overall performance.

## 10. Recommendations

The Snake method introduces a Multiscale approach for edge detection by using active Contour model for efficiently detecting the iris region for use in the future extraction stage. Once this is done, a combined feature extraction scheme using Mat-lab algorithm components to extract all texture information from orientation in horizontal and vertical details is employed to obtain useful results.

## 11. REFERENCES

Adeboye, K. R. & Ezeako, L.N. (2007). Numerical Algorithm for Digital Image Enhancement and Noise Minimization, *Global Journal AS* 7 (1), 63-68

Adeboye, K. R., Lanlege D. I. & Gana, U. M. (2013). Musculoskeletal Magnetic Resonance Imaging Segmentation Using Finite Element Method *Journal of Nigeria Association of Mathematical Physics* 25(2), 65-72.

Adeboye, K. R., Yahaya, Y. A. & Lanlege, D. I. (2013). Effective way of Noise Smoothing during Image Processing Using Multiscale Proportional IntegralDerivative (PID) Filter Controller. *International Research Journal Science and Engineering T*echnology 2(2), 17-24.

Ezeako, (2005). Pattern Recognition: An Enhanced Sub-Array Algorithm for Processing of Large Data-Set Problems in a Transform Domain *Ph.D Thesis* Federal University OF Technology Minna 73-93.

Goswami, M. K. (1999). Constrained Image Restoration and the Recovery of Discontinuities. IEEE Transition. PAMI, 3 (14), 367 – 383.

Kong,W &Zhang, D (2001).Accurate Iris Segmentation Based on Novel Reflection And Eyelash Detection Model Proceeding of 2001 International Symposium on Intelligent Multi-Media, Video and Speech Processing Hong Kong in China

Laurent, J.C. & Cohen, A.K. (2011). *Fundamentals of Wavelet: Theory, Algorithms and Application.* New York, John Wiley& Sons, 409-431.

Mallat, S. & Zhong, S.(1992) Analysis and Machine Characterization of Signal from Multiscale 710-732.

Manjunath & Ma,L. (2003). Personal Identification Based on Iris Texture Analysis *IEEE Transaction on Pattern Analysis and Machine Intelligence*(25), 1519-1533

Rudin L., Osher S. J. & Fatemi E. (1992). Nonlinear Total Variation Based Noise Removal Algorithms Physical D., 60, 259 – 268.

Abacus (Mathematics Science Series) Vol. 44, No 1, Aug. 2019

# A NOTE ON STRONGLY INVARIANT SUBGROUP

**by**

**U. Adamu & M. A. Ibrahim**

*Department of Mathematics, Ahmadu Bello University, Zaria*

*uadamu@abu.edu.ng & amibrahim@abu.edu.ng*

**Abstract.**

*In this paper,we formulate some results on strongly invariant subgroup. We show that diagonal subgroups are not strongly invariant, the union of a strongly invariant subgroup of a group $G$ and a direct factor of $G$is not strongly invariant.We establish that every subgroup $A$ of a torsion group $G$ is strongly invariant if $A[n]$ is strongly invariant in $A$. The union and the intersection of a torsion part of a mixed group are strongly invariant. We finally show that every cyclic group of prime order is strongly invariant simple.*

## 1. Introduction

The concept of fully invariant subgroup was introduced by F. Levi under the German namevollinvariant in[1].Fully invariant extending property (FI-extending property) for abelian groups was studied in[2], where it was proved thata torsion group has the FI-extending property if it is a direct sum of a divisible group and separable $p$-groups, every summand of a group with theFI-extending property enjoys theFI-extending property, a mixed abelian group has theFI-extending property if it is a direct sum of torsion and torsion-free Abelian group, both with the FI-extending property.

Chekhlov in[3], described the intermediately fully invariant subgroup (ifi-subgroup) of divisible, torsion and torsion-free groups, it is shown thatsum of ifi-subgroups is againifi-subgroup.The intersection of the subgroup $N$ with the subgroup $H$ of a group $G = H \oplus K$ such that$N = (N \cap H)\oplus(N \cap K)$ is an ifi-subgroup in $H$. Furthermore, in a torsion group $G$a subgroup $H$ is intermediately inert in $G$ if every $p$-component of $H$ is intermediately inert in $p$-component of $G$, and finally, every homogeneous separable torsion-free group ofrank $\geq 2$ isifi-simple.

The notion of strongly invariant subgroups ofAbelian groupswas introduced and studied in [4] as an extension of fully invariant subgroups, and therein, it was shown that ina torsion group $G$a subgroup $A$ is strongly invariant if $p$-componenet of $A$ is strongly invariant in$p$-component of $G$. For a reduced $p$-group the only strongly invariant subgroups are the subgroups $G[p^n]$. The intersection of the strongly invariant subgroup $N$ and the subgroup $H$ of a group$G = H \oplus K$ such that $N = (N \cap H) \oplus (N \cap K)$ is strongly invariant in $H$.For atorsion-free group, a subgroup $A$ is not strongly invariant if it contains free direct summand. It was also discovered that rank 2 torsion-free group has no cyclic strongly invariant subgroup. The torsion part of subgroup $N$ of a mixed group $G$ is strongly invariant in torsion part of $G$ if it is strongly invariant in $G$ and infinite cyclic subgroups of $G$ and a subgroup that contains a free direct summand are not strongly invariant.More results like; a $p$-group is fully invariant simple if it is elementary, a torsion group is strongly invariant simple if it is an elementary$p$-group, genuine mixed groups are not strongly invariant simple and any torsion-free divisible group is strongly invariant simple are established.

The strongly invariant subgroup of torsion-free groups was studied in [5].Some results like; in a divisible torsion-free group every fully invariant subgroup is strongly invariant, every homogeneous separable torsion-free group is strongly invariant simple, every strongly invariant subgroup coincides with some direct summand of the group, and the sum of strongly invariant subgroups is again strongly invariant subgroup.

This paper extend some of the results in[4]. We study the strongly invariant subgroup of the direct product of two subgroups, the strongly invariant subgroup of torsion group, mixed group and in particular, those of strongly invariant simple group and obtain some results.

## 2. Basic Definitions

**Definition 1. (Fully invariant subgroup)**

A subgroup $B$ of a group $A$ that is carried into itself by every endomorphism of $A$ is said to be a fully invariant subgroup of $A$. [6].

*Example 2.1.*Commutator subgroups are fully invariant, in a cyclic group every subgroup is fully invariant, and every group is fully invariant as subgroup of itself.

**Definition 2. (Strongly invariant subgroup)**

A subgroup $N$ of a group $G$will be called strongly invariant in $G$, if$f(N) \leq N$ for every group homomorphism $f : N \longrightarrow G$. [4].

*Example 2.2.*Normal Sylow-subgroup, normal Hall subgroup are strongly invariant and the center of the quaternion group$Q_8$ is a strongly invariant subgroup of$Q_8$.

**Definition 3. (Torsion group)**

An Abelian group is called a torsion or periodic group if every element of $A$ is of finite order.[6].

*Example 2.3.*Every finite group is periodic.

**Definition 4. (Torsion-free group)**

An Abelian group is called a torsion-free if all its elements, except for 0, are of infinite order. [6].

*Example 2.4.*The set of integers under addition is a torsion-free group.

**Definition 5.(Mixed group)**An Abelian group is called mixed group if it contain both nonzeroelementsof finite order and elements of infinite order.[*6*].

*Example 2.5.*The group$□ = □_□ \oplus □ = \{(□', □),\ □' \in □_□$ and $□ \in □\}$ is a mixed group.

**Definition 6. (Strongly invariant simple group)**

An Abelian group is said to be strongly invariant simple if it has non nontrivial strongly invariant subgroup.[*5*].

*Example 2.6.*The group $□ = □_2 \oplus □_2$ is strongly invariant simple group.

**Definition 7. (Direct factor)**

A subgroup □ of a group □ is called direct factor of □ if there is a subgroup □ of a group □ such that □ is the internal direct product of □ and □. [*7*].

*Example 2.7.*Let $□ = □_6 = \{0, 1, 2, 3, 4, 5\}$ and $□ = \{0, 2, 4\}$be a subgroup of □ then □ is a direct factor of □ since there is $□ = \{0, 3\}$in □ with $□ = □\,□$ and $□ \cap □ = \{□\}$.

**Definition 8. (Diagonal subgroup)**

Let $□ = □ \oplus □$ be a direct product of two isomorphic groups □ and □ then a subgroup □ of □is called diagonal subgroup if $□\,□ = □ = □\,□$and $□ \cap □ = □ = □ \cap □$. [*7*].

*Example 2.8*Let □ = {□, □, □, □} be a Klein four-group and let□ = {□, □}and □ = {□, □}be two subgroups of □ such that □ = □ ⊕ □, then a subgroup □ = {□, □} is a diagonal subgroup of □.

## □. Some Existing Results

**Theorem** □. □.Fully invariant direct factors are strongly invariant.[*4*].

**Theorem** □. □.If a group □ = □ ⊕ □ and □ is fully invariant subgroup of □, then□ = (□ ∩ □) ⊕ (□ ∩ □). [*6*].

**Theorem** □. □. Any sum of strongly invariant subgroups is a strongly invariant subgroup.[*5*].

**Theorem** □. □.Let □ be strongly invariant subgroup of a group □ = □ ⊕ □, then□ = (□ ∩ □) ⊕ (□ ∩ □) and □ ∩ □,□ ∩ □are strongly invariant in □ and □ respectively. Conversely, if □$_{1}$ and □$_{1}$are strongly invariant subgroups of □ and □ respectively, then□$_{1}$ ⊕ □$_{1}$is strongly invariant in □ if and only if for every □ : □$_{1}$ ⟶ □, □(□$_{1}$) ≤ □$_{1}$and for every □ : □$_{1}$ ⟶ □, □(□$_{1}$) ≤ □$_{1}$. [*4*].

**Lemma** □. □. In any group □, for any positive integer □, the subgroup□[□] = {□ ∈ □ : □ □= *0*} is strongly invariant in □. [*4*].

**Theorem** □. □.Let □ be a subgroup of a torsion group □. Then □ is strongly invariant subgroup of □ if and only if for every prime *p*, □$_{□}$ is strongly invariant in□$_{□}$.[*4*].

**Theorem** □. □.Let □ be a subgroup of a mixed group □. Then □(□) is strongly invariant subgroup of □(□) if and only if □(□) is strongly invariant subgroup of □.[*4*].

**Theorem** □. □. [*4*].

i. A □-group □ is fully invariant simple if and only if it is elementary.
ii. Genuine mixed groups are not strongly invariant simple.
iii. A torsion group is strongly invariant simple if and only if it is an elementary □-group.

## □. Main Results

**Theorem** □. □.Let □ be strongly invariant subgroup of a group □ = □ ⊕ □, and□ = (□ ∩ □) ⊕ (□ ∩ □) then □ ∪ □ and□ ∪ □are not strongly invariant in □ and □ respectively if and only if □ ∩ □ ≠ {□} and □ ∩ □ ≠ {□}.

**Proof.** Suppose □ ∪ □ is strongly invariant in □ then □ ∪ □ ≤ □ this implies □ ⊆ □. But since □ ∩ □ ≠ {□} there exists □ ∈ □ ∩ □ such that □ ∉ □ and so □ ⊈ □ which is a contradiction. Therefore, □ ∪ □is not strongly invariant in □. Similarly, □ ∪ □is not strongly invariant in □.Conversely,if □ ∩ □ = {□} and □ ∩ □ = {□}then □ ∪ □ and□ ∪ □are strongly invariant in □ and □ respectively, which is a contradiction. Hence, □ ∩ □ ≠ {□} and □ ∩ □ ≠ {□}.

**Theorem** □. □.Let □ = □ ⊕ □ be the direct product of two isomorphic groups, then the diagonal subgroup □ of □ is not strongly invariant.

**Proof.** Suppose □ is strongly invariant subgroup of □ then □ = (□ ∩ □) ⊕ (□ ∩ □) since□ is a diagonal subgroup of □, we have □ □= □ = □ □and □ ∩ □ = □ = □ ∩ □ and so□ ≠ (□ ∩ □) ⊕ (□ ∩ □).

**Theorem** □. □.Let □ be a subgroup of a torsion group □. Then □ is strongly invariant subgroup of □ if and only if for any positive integer *n*, □[□] is strongly invariant in □[□].

**Proof.** *Necessity*. For any positive integer □, let □ ∶ □[□] ⟶ □[□] be a homomorphism then □(□[□]) ≤ □[□]. Since □[□] ≤ □ and □[□] ≤ □ we can extend the mapping□ ∶ □ ⟶ □ and by hypothesis □(□) ≤ □. Thus, we have □(□[□]) ≤ □ and so□(□[□]) ≤ □ ∩ □[□] = □[□].
*Sufficiency*. Let □ ∶ □ ⟶ □ be a group homomorphism. Since □[□] is a subgroup of □ and □[□] is a subgroup of □ we can restrict the mapping to □ ∶ □[□] ⟶ □[□] and by hypothesis□(□[□]) ≤ □[□] for any positive integer □. Therefore, □(□) ≤ □.

**Theorem** □. □.Let □ and □ be subgroups of a mixed group □ such that □ ≤ □ ≤ □. If □(□)is strongly invariant in □(□), then □(□) ∩ □(□) is strongly invariant in □.

**Proof.** Let□(□)be strongly invariant subgroup of □(□) then □(□) ≤ □(□) and so□(□) ∩ □(□) = □(□). From theorem 3.7 we infer that □(□) ∩ □(□) is strongly invariant in □.

**Theorem** □. □.Let □ and □ be subgroups of a mixed group □. If □(□) and □(□) are strongly invariant in □ then □(□) ∪ □(□) is strongly invariant in □ if and only if □(□)and □(□) are comparable.
**Proof.** Let □(□) ∪ □(□)be strongly invariant in □ then □(□) ∪ □(□) ≤ □.If □(□)and □(□) are not comparable we have □(□) ∪ □(□) ≰ □, which is a contradiction. Therefore,□(□)and □(□) are comparable. Conversely, Suppose □(□)and □(□) are comparable such that □(□) ⊆ □(□) then □(□) ∪ □(□) = □(□) and so □(□) ∪ □(□) is strongly invariant in □. Similarly, if □(□) ⊆ □(□) also□(□) ∪ □(□) is strongly invariant in □.

**Theorem** □. □.Every cyclic group of prime order □ is strongly invariant simple.

**Proof.** Let □ be a cyclic group with a generator □ ∈ □ then ∀ □, □ ∈ □, ∃ □, □ ∈ □ such that □ = □ □ and y = m□ it follows that

□ + □ = □ □+ □ □= □(□ + □) = □(□ + □) = □ □+ □ □= □ + □.

Hence, □ is abelian.
Let □ be any subgroup of □. Since □ is cyclic for every homomorphism □ ∶ □ ⟶ □, there exists □ ∈ □ such that ∀ □ ∈ □, □(□) = □□ ∈ □ this implies □is strongly invariant.But, since □(□) = □ by Lagrange's theorem □(□)|□ and so □ is a trivial subgroup. Hence □ is strongly invariant simple.

## □. Conclusion and Recommendation

In this note we discussed the conditions for a subgroup □ of a group □ which is the direct product of its two subgroups to be strongly invariant. The concept of torsion Abelian group, mixed Abelian group and strongly invariant simple Abelian group have been discussed and some related results were obtained. We recommend for the investigationof theunion and intersection of strongly invariant subgroups of torsion-free group, torsion group and strongly invariant subgroups of non Abelian groups.

**References**

F. Levi, Uber die Untergruppen der freien Gruppe, *Math. Zeit.* **37**, 90−99 (1933).
G. F. Birkenmeier, G.Clugreanu, L.Fuchs, and H. P.Goeters,Fully invariant extending property for abelian groups, *Communications in Algebra*, 29:2,673−685 (2001).
A. R. Chekhlov, Intermediately fully invariant subgroups of Abelian groups,*Siberian Mathematical Journal*, vol. 58, No. 5, pp. 907−914, (2017).
G. Călugăreanu, Strongly invariant subgroups,*Glasg. Math. J*.57 (2), 431−443 (2015).
A. R. Chekhlov, On strongly invariant subgroups of Abelian groups, ISSN 0001−4346, *Mathematical Notes*, vol. 102, No. 1, pp. 105−110 (2017).
L. Fuchs, *Infinite Abelian groups*, vol. 1 (Academic Press, 1970).
R. Schmidt, *Subgroup Lattices of Groups*, de Gruyter Expositions in Mathematics (1994).